SLAC-PUB--5925

DE93 004007

Preliminary Test Results From a Telescope of Hughes Pixel Arrays at FNAL*

J. G. Jernigan, J. Arens, and D. Vezie
Space Sciences Laboratory,University of California, Berkeley, CA 94720

S. L. Shapiro
Stanford Linear Accelerator Center, Stanford University, Stanford, CA 94309

T. Collins
Hughes Aircraft Company, Carlsbad, CA 92009

J. Krider
Fermi National Accelerator Laboratory, Batavia, IL 60510

P. Skubic
University of Oklahoma, Norman, OK 73019

ABSTRACT

In December of 1991 three silicon hybrid pixel detectors each having 256 × 256 pixels 30 μm square, made by the Hughes Aircraft Company, were placed in a high energy muon beam at the Fermi National Accelerator Laboratory. Straight tracks were recorded in these detectors at angles to the normal to the plane of the silicon ranging from 0 to 45°. In this note, preliminary results are presented on the straight through tracks, i.e., those passing through the telescope at normal incidence. Pulse height data, signal-to-noise data, and preliminary straight line fits to the data resulting in residual distributions are presented. Preliminary calculations show spatial resolution of less than 5 μm in two dimensions.

1. INTRODUCTION

An architecture appropriate for high energy charged particle detection is that of a hybrid [1-4]. The charged particle detector and the readout electronics are constructed as two separate silicon chips, each optimized for its specific function. The two chips, indium bump bonded together, then provide the basic building block for the construction of a detector array.

The choice of the hybrid design (viz., one in which each diode of the detector array is bonded to an independent amplifier readout circuit on a mating VLSI chip via an array of aligned indium metal bumps that cold weld under pressure to form ohmic contact), allows for additional flexibility in the selection of detector and readout electronics. For instance, a change in the leakage current specification of the detector array will not affect the readout electronics, nor will a change in the VLSI chip oxide thickness to accommodate a radiation hardness specification affect the detector array. Figure 1 is a schematic representation of a silicon PIN diode array hybrid.

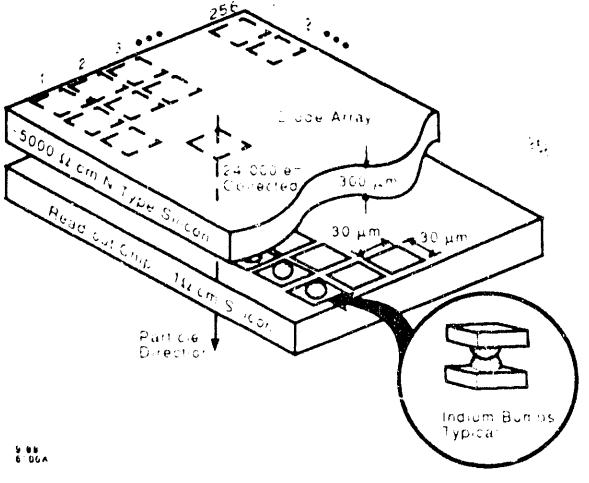

Figure 1. Schematic representation of a hybrid Silicon PIN Diode detector

* Work supported by Department of Energy contract DE-AC03-76SF00515.

Invited talk presented at the International Conference on B Factories: The State of the Art in Accelerators, Detectors and Physics, Stanford, CA, April 6-10, 1992

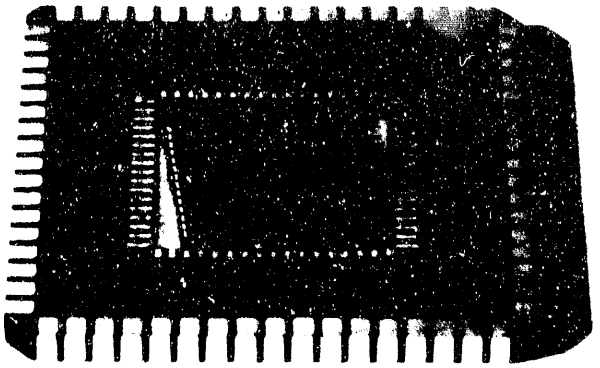

Figure 2. Photograph of 256 × 256 silicon hybrid similar to the ones used in this measurement.

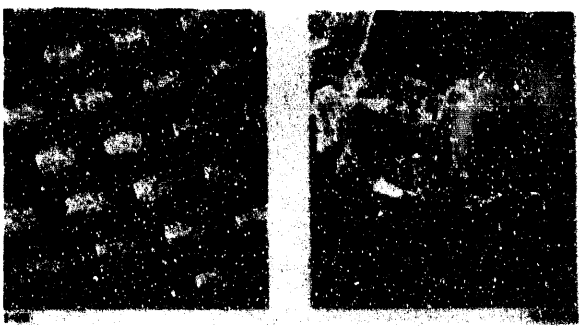

Figure 3. Microphotograph of an array of indium bumps prior to the bonding process.

SILICON HYBRID ARRAYS

Development of hybrid vertex detectors has been the goal of the authors since late 1984. To this end 256 × 256 hybrid arrays having 30 μm square pixels have been designed and fabricated. The sensor arrays were fabricated by Micron Semiconductor and the readout arrays by Hughes Aircraft. Figure 2 is a photograph of the 256 × 256 hybrid array fabricated by Hughes Aircraft Company, similar to the ones used in this measurement. The indium bump bonding done by Hughes Aircraft employed bumps measuring under 15 μm in diameter. Figure 3 is a microphotograph of an array of indium bumps prior to the bonding process.

THE SET UP

The test was set up in the New Muon Facility at Fermilab. A beam of muons of approximately 450 GeV/c momentum was available to a number of experimenters in this area. The area was off-limits for personnel access

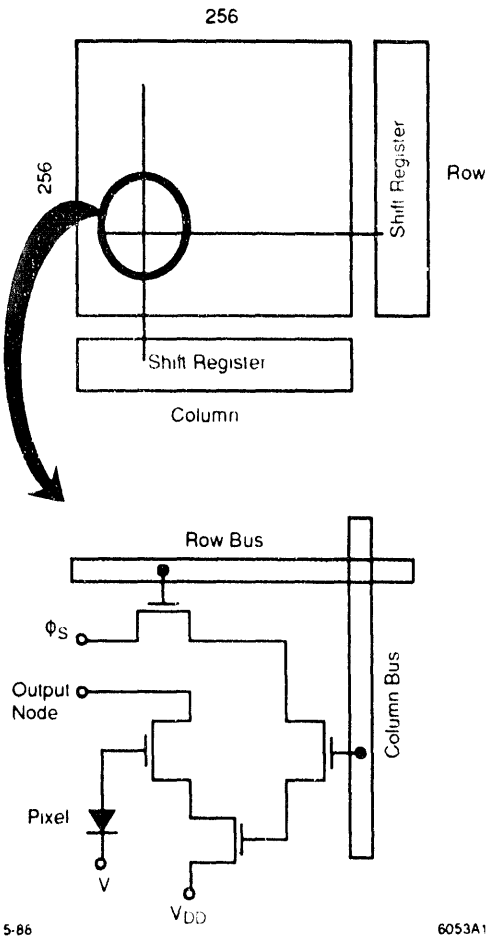

Figure 4. A schematic representation of the readout architecture of the 256 × 256 array and of the MOSFET single cell.

due to a perceived radiation hazard, so the entire experiment had to be operated and controlled from outside the radiation fence. Apparatus to place our experimental gear into the beam line for the test, and remove it so that changes could be made in orientation was designed, built and installed by the Fermilab staff under the direction of one of the authors. This same apparatus enabled the placement of our test gear in various places within the broad muon beam, so that data could be taken at a number of different intensities.

Cooling of our apparatus was achieved by the inclusion of an air conditioning unit within the Faraday cage. There was little in the way of control of the temperature, but the unit worked well in that the operating temperature settled out at about 0°C when the unit was turned full on. Even the slight (1 to 2°C) temperature shifts made noticeable changes in pedestal values, but these were easily removed by the median filter to be described later.Each of the silicon hybrids was mounted on a stitch-wire board containing a socket for the 68-pin

leadless chip carrier and a filter for each of the DC levels necessary to run the detector The chip carrier cards were mounted on a small optical bench with each card able to be moved along the bench while retaining its orientation with respect to the other detectors. The detector which was mounted between the other two had an additional degree of freedom in that rotation about a vertical axis was permitted. During the course of this test run, the center detector was rotated from its normal position through a number of angles from 0 to 45°. The distance between the detectors was altered slightly to permit these changes in angle.

DESCRIPTION OF THE DATA ACQUISITION SYSTEM

Figure 4 is a simple schematic of the readout addressing architecture of the 256 × 256 array and of the MOSFET single cell itself. This array contains only two output nodes for the entire chip.

Figure 5 is a block diagram of the high energy physics data acquisition system. A Sun Microsystems SPARC Station 1^+ workstation controls a system housing a Sun 1/E CPU, amplifiers, ADCs, digital signal processors, PECK bus controller, and a clock generator. The digital signal processor is the Motorola DSP56001. This device acquires data at a rate of 10 MIPS, processes it, and passes it, via the PECK bus controller (also based on the DSP56001) to the Sun 1/E. The SUN 1/E and half of the PECK bus controller reside in a VME crate, while the balance of the electronics—including the other half of the controller—reside in a special enclosure that employs a dedicated bus called the PECK bus.

A data acquisition and display software package has been written. The operating system is UNIX, the DSPs have been programmed in assembly language, and the Sun 1/E programmed in C.

The data were acquired at a rate of 2.4 μs per pixel. The three detectors, using six readout channels of electronics were read out in parallel; thus it required only 72 ms to store the data to the on-board buffers. The full readout cycle took about one minute per read, however, as the system transfer rate to the host was limited by bus loading. The read cycle was not initiated by, nor was it necessarily synchronized with, the beam. Thus, many read cycles did not contain any data. The test nevertheless resulted in more than enough data at each of the various settings. The beam intensity was constant over the run, but the telescope was placed at various locations yielding data rates of from 50 to 400 tracks per frame.

DATA ANALYSIS AND PRELIMINARY RESULTS

The data being presented here is the first to be analyzed by our group, and consists solely of the "straight through" muons. That is, those particles which transit the telescope normal to each of the three detectors.

Figure 6 is a log plot that combines two spectra. The spectrum on the left, the large spike, is a sample of the noise inherent in this system, while the smaller peak on the right is the signal caused by the passage of the charged particle.

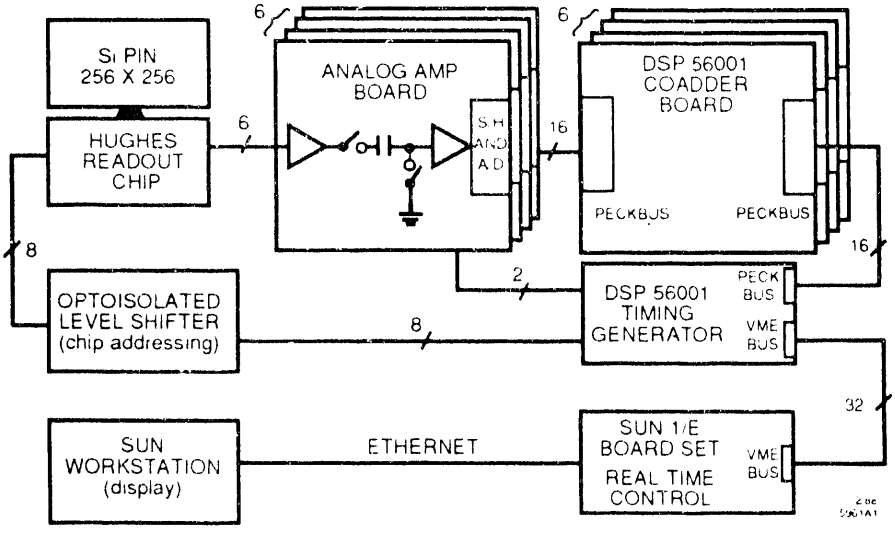

Figure 5. A block diagram of the high energy physics data acquisition system used for this measurement.

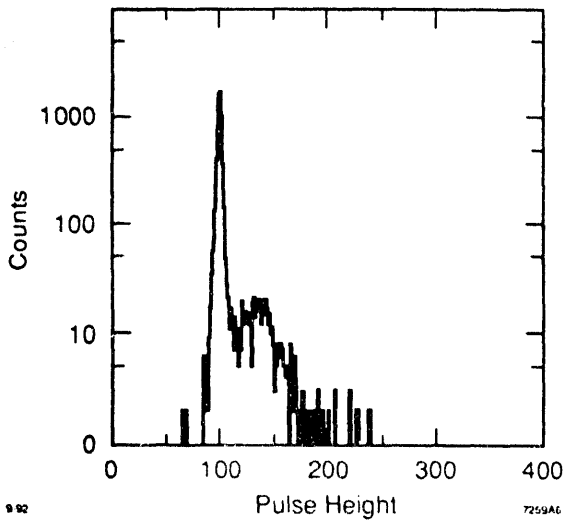

Figure 6. A log plot of the pulse height from the detector from which an estimate of signal-to-noise per pixel can be achieved..

The data filter identifies a "HIT" when the pulse height in a pixel exceeds the minimum threshold (about 3000 e^- rms equivalent). This number is entered into the spectrum. Only the PEAK pixel is entered into this plot. It should be mentioned here that these entries are not necessarily part of a track. The beam contains a large number of high energy gamma rays, which at this point have not yet been removed from the data.

To identify the noise associated with this hit, the pulse height values in each of the three pixels defining the four corners of a 5×5 square about the hit pixel are entered (a total of 12 entries in all). The signal-to-noise ratio for a single pixel can be approximated from this curve to be about 45-50:1, where the noise is taken to be the width σ of the noise spike, and the signal is taken to be the most probable value of the signal peak. As the signal here is only the PEAK pixel, it contains only about 60% of the deposited charge. The final signal-to-noise will be calculated later after summing all of the charge in a cluster.

As of this writing, no systematic effort has been made to understand the following systematic effects.

* Only zeroth order corrections for gain variations between even and odd columns have been implemented. Recall that even columns are read out though a separate analog chain from the odd columns,
* Accounting for cross-coupling corrections (the small remnant of charge that remains on a column's read node after detection of a significant hit on a pixel) should be subtracted from the second-to-be-read pixel.
* Devising an optimum clustering algorithm. Presently, all the pixels in a 3×3 square about the pixel with the highest pulse height per hit are combined to form a sum, which is then identified with the charge left behind by the passage of the charged particles. This results in a noise-per-sum equal to three [9] times the noise on a single pixel.

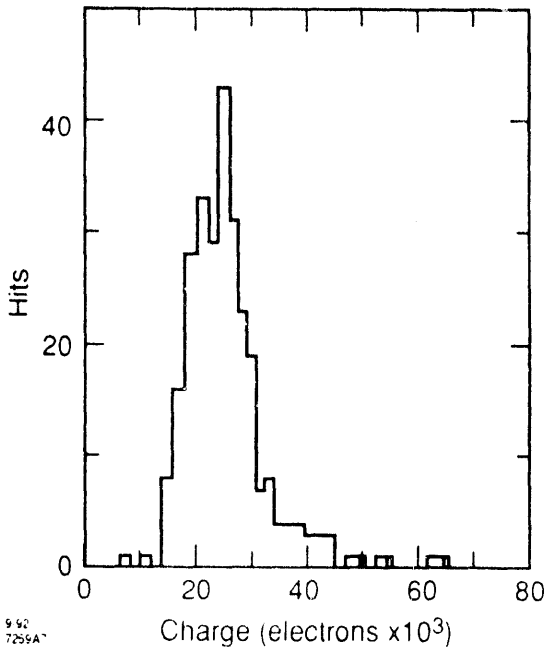

Figure 7. The pulse height distribution of hits from 450 GeV/c muons traversing three planes of silicon at normal incidence

Pedestal variations are properly removed by subtracting from each pixel a median filter comprised of the median of the previous five frame's value for that pixel. In this fashion, temperature and time variations are properly removed.

Figure 7 is a pulse height distribution of hits within each hybrid detector. For each hit, which resides on one of the fitted straight lines, the pulse height from the pixel with the highest pulse height is combined with the pulse heights of all of the pixels that border it, viz., those contained in a 3×3 square around it, to form the sum plotted in the figure.

PRELIMINARY VALUES FOR SPATIAL RESOLUTION.

In an attempt to determine spatial resolution, straight lines were fit to the data, and residual distribution plotted. These are shown in Fig. 8.

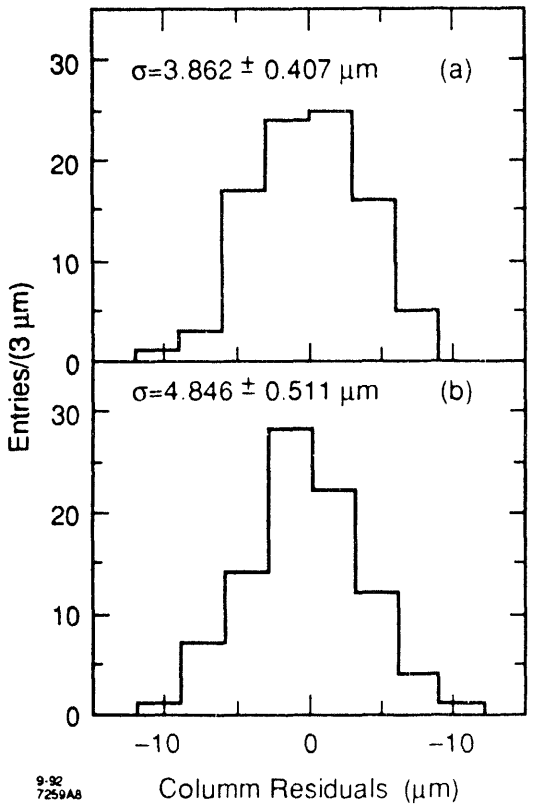

Figure 8. Row (a) and column (b) residuals plots to the straight line fits to hits in the three detectors of the telescope, demonstrating the superb spatial resolution obtainable.

Determining the location of the passage of a particle through a pixel requires the use of an algorithm that makes use of the pulse height of the PEAK pixel (that one which has the highest pulse height per hit) and its neighbor in both dimensions. This algorithm was first discussed in [3] and will be mentioned again here.

In our geometry, particles enter the device on the cathode of the PIN diode, the side farthest from the bump bonds. Thus, much of the charge collected must drift across the entire depletion distance of 300 μm. The charge cloud, spread by scattering of the initial radiation and by diffusion, will have a finite lateral size. If a particle were closer to the edge of a pixel than to the center, one would expect charge to be shared by adjacent pixels. On average, we see charge spread over two to four pixels of the nine pixels in a 3 × 3 array.

Detailed analysis of a set of pixels near a particle hit allows calculation of four quantities: signal-to-noise, noise, size of the charge cloud, and spatial resolution.

In Fig. 9(a), a schematic of a 5 × 5 region centered on a particle hit is shown. The pixel with the maximum signal, located at (0,0), is labelled "PEAK." The pulse height of its signal is referred to as P. Nearby pixels are located by offsets between −2 and +2. Each pixel in the 5 × 5 region has its zero set by the use of the temporal median filter, which essentially rejects previous hits.

Further, in analyzing a particular hit, the outer border of 16 pixels is used to define two additional constants that are subtracted from the inner 9 pixels to remove any

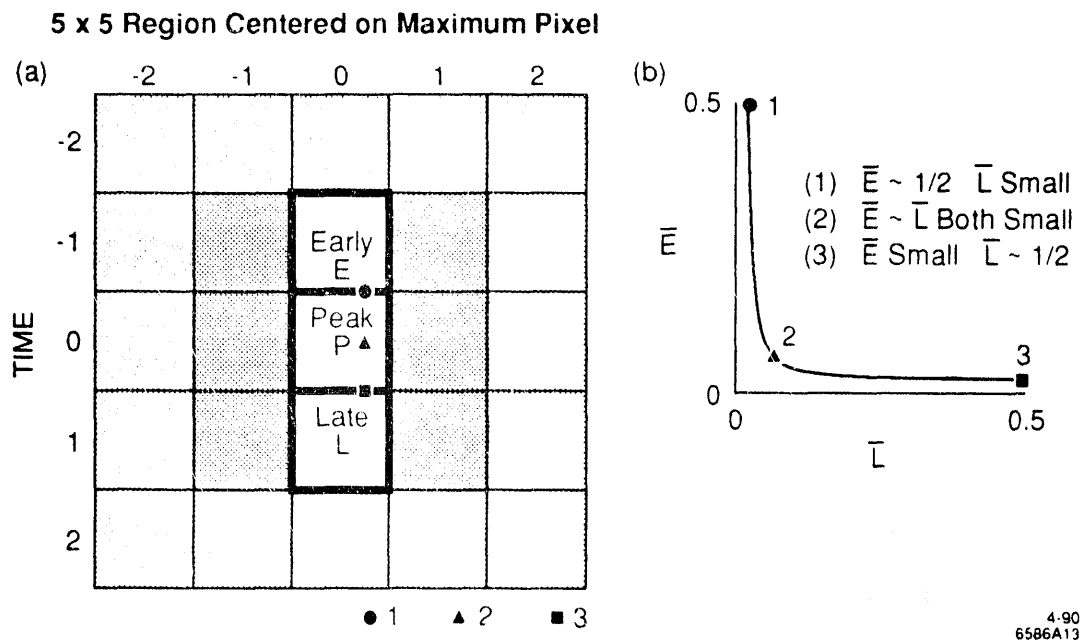

Figure 9. A schematic of (a) a 5 × 5 pixel region centered on a particle hit, and (b) the $\bar{E}$ versus $\bar{L}$ planes indicating the result of various hypothetical incident positions of a particle within the central pixel.

systematic offset that arises because of the separation in time between the measurement of the background frames and the frame containing the particle hit. In this last subtraction, the pixels in the first and fifth column are used to correct those in the third column, while the four pixels at the extremities of the second and fourth column are used to correct the second and fourth column.

The direction of time in Fig. 9(a) refers to the sequence of the readout of the pixels. In this device, columns are read out in parallel; thus, the five pixels in the row labeled −2 at the top of the figure are read out first, with sequential readout, by row, from −2 to +2 on the time axis. For convenience, the pixel just above the PEAK is labelled "EARLY" and its contents referred to as E, while the pixel just below the PEAK is labelled "LATE" and its contents referred to as L. E, P, and L are used to derive the E and L ratio from the relation:

$$E = \frac{E}{(E+P+L)} \quad \text{and} \quad L = \frac{L}{(E+P+L)}$$

Figure 9(b) is a schematic plot in the E versus L plane of what should happen if a particle were to hit different parts of the central pixel. Possibilities 1, 2, and 3 are indicated in the central pixel, with their corresponding results shown in Fig. 9(b). The position of possibility 2 will be close to or far from the origin, depending on the size of the charge cloud.

Figure 10 is a scatterplot of the data from this test run. It can be seen that the trend of this data to fall near the axes, as explained in Fig. 9(b), is as expected. Since much of the careful systematic analysis of the data (such as gain corrections, etc.) remains to be done, not too much will be made of this effect at this time. However, an analysis of the density of points in this scatterplot leads to the following interpolation algorithm:

For the rows,

if $R_x < 0.3$, then $dx = 1.33 \times R_x$

if $R_x > 0.3$, then $dx = 0.5 \times (R_x + 0.5)$

where R_x = Larger Neighbor / SUM_x and

SUM_x = PEAK + the neighbors above and below.

For the columns, the same formulae apply

if $R_y < 0.3$, then $d_y = 1.33 \times R_y$

if $R_y > 0.3$, then $d_y = 0.5 \times (R_y + 0.5)$

where R_y = Larger Neighbor / SUMy and

SUM_y = PEAK + left and right neighbors

Note that these algorithms bound dx and dy (the fractional distance from the center of the pixel) at 0.5, since R_x and R_y are bounded by 0.5. That is, the largest

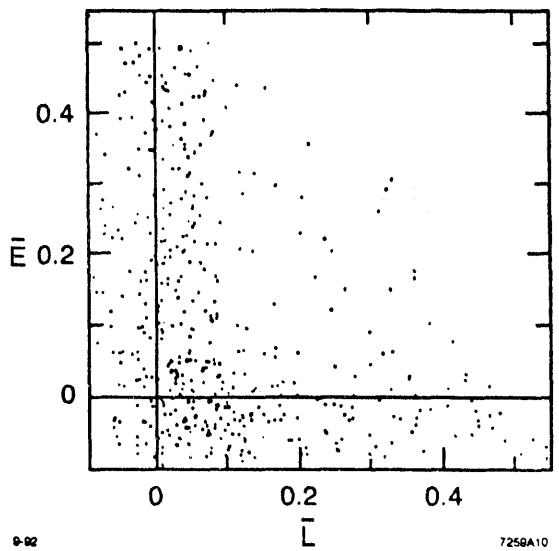

Figure 10. A Scatterplot of charge sharing for high energy muons incident on one of the 256 × 256 detector planes of the telescope displaying the expected behavior.

amount of charge to be found in a neighbor is one half. If it were larger it would become the PEAK.

These algorithms can be used to establish the x and y position of each of the hits in each of the detectors, and then fit these points to straight lines. Gamma rays and spurious hot pixels will not participate in a straight line fit, and so are eliminated here. From the plots of the row and column residuals in Fig. 8, it is possible to determine a first estimate of the spatial resolution of the 256 × 256 detector hybrids. The row rms is 3.9 ± 0.4 μm and the column rms is 4.8 ± 0.5 μm.

SUMMARY/CONCLUSIONS/PROJECTIONS

Three 256 × 256 Hughes arrays have been organized into a telescope and placed in a high energy muon beam at FNAL. A noise level of less than 300 e^- (rms) has been observed at 0°C operation. Spatial resolution of better than 5 μm in both the x and y dimensions has been measured for normal incidence.

A number of important systematic studies remain to be done that will surely increase the spatial accuracy of this measurement. Similarly, an analysis of the data involving muons traversing the silicon at other than normal incidence is in progress. These data promise interesting results. It is hoped that they will not only show good spatial resolution, but that they will indicate the capability of actually measuring the track angle by its passage through a single plane of silicon. The analysis is expected to be complete by the end of 1992.

REFERENCES

[1] S. Shapiro, J. Arens, W. Dunwoodie, S. Gaalema, J. G. Jernigan, "Silicon PIN Diode Array Hybrids for Charged Particle Detection," Nucl. Instrum. Methods **A275** 580 (1989).

[2] S. Gaalema, J. Arens, W. Dunwoodie, J. G. Jernigan, G. Kramer, and S. L. Shapiro, "Silicon PIN Diode Hybrid Arrays for Charged Particle Detection: Building Blocks for Vertex Detectors at the SSC," Proc. Int. Industrial Symposium on the Supercollider, New Orleans, LA, 1989, p.173.

[3] J. G. Jernigan, J. F. Arens, T. Collins, J. Herring, G. Kramer, S. L. Shapiro, C. Wilburn, "Performance Measurements of Hybrid Pin Diode Arrays," presented at the Int. Industrial Symposium on the Supercollider, Miami Beach, FL, 1990, SLAC--PUB-5211.

[4] S. Shapiro, "Silicon PIN Diode Array Hybrids as Building Blocks for a Vertex Detector at an Asymmetric B-Factory", SLAC-PUB-5353 (1990); see also Proc. of the Workshop on Physics and Detector Issues for a High Luminosity Asymmetric B-Factory, SLAC-373 (1990).

END

DATE FILMED

2/2/93